

An assessment of the interactions between diclofenac sodium and ammonio methacrylate copolymer using thermal analysis and Raman spectroscopy

Péter Sipos^a, Mária Szűcs^a, András Szabó^b, István Erős^a, Piroska Szabó-Révész^{a,*}

^a Department of Pharmaceutical Technology, University of Szeged, Eötvös str. 6, H-6720 Szeged, Hungary

^b Department of Organic Chemical Technology, Budapest University of Technology and Economics, Műegyetem rakpart, H-1111 Budapest, Hungary

Received 16 July 2007; received in revised form 4 October 2007; accepted 6 October 2007

Available online 13 October 2007

Abstract

The objective of the work was to assess the possible interactions between the model drug diclofenac sodium (DS) and the water-insoluble ammonio methacrylate copolymer (AMC). Films with different drug/polymer ratios were therefore prepared by the solvent casting method and investigated as a preformulation study towards sustained release microparticles. Differential scanning calorimetry (DSC) and thermogravimetric analysis (TGA) were used to investigate the dispersed/dissolved state of the DS in the preparation, the thermal stability and the properties of DS-containing AMC films; and Raman spectroscopy was used to confirm the possible interactions between DS and AMC. Thermoanalytical studies confirmed that the DS could behave as a plasticizer, which was indicated by decreasing glass transition temperature (T_g) of the AMC, depending on its dispersity level in the AMC matrix. Partially solid solutions were formed at DS/AMC ratios of 1:12, 1:8 and 1:6. The DS was mainly crystalline at DS/AMC ratio of 1:4, while it remained crystalline at a ratio of 1:2. The Raman spectra confirmed that none of the major structural changes revealed any significant difference, which can indicate a strong ionic interaction between the DS and the AMC. The investigations provided good facilities for the selection of a DS/AMC ratio, in the preformulation study of the microsphere preparation process, in conformity with the therapeutic aim.

© 2007 Elsevier B.V. All rights reserved.

Keywords: Preformulation; Solvent casting method; Diclofenac sodium; Ammonio methacrylate copolymer; Thermoanalysis; Raman spectroscopy

1. Introduction

Microparticles of polymer matrix-based spherical solids comprise two main groups: microcapsules (a drug core and a polymer coat) and microspheres (dispersed/dissolved drug in the polymer matrix). Before preparing them, it is necessary to identify the state of the drug in the polymer and the compatibility of the components. This work involved the characterization of the dispersed/dissolved state of the drug and determination of the possible interactions between the drug and the polymer, using, among other methods, thermal analysis and Raman spectroscopy. Thermal investigations are important before high-

temperature (i.e. spray-drying) preparation methods are applied. Differential scanning calorimetry (DSC) and thermogravimetry (TGA) allow an understanding of the thermal behaviour of the components and the dispersity of the active agent; these methods were therefore used to investigate the properties of the drug-containing films. The films were characterized by the glass transition temperature (T_g) and the melting endotherm (T_m). Raman spectroscopy is an effective analytical method for the characterization of complex dosage forms in pharmaceutical technology [1,2], and differentiation of the crystalline form of the materials [3]. This method was applied to detect the changes in the drug–polymer structure and to establish the interactions between the drug–polymer chain segments, by subtraction of the Raman spectra.

Diclofenac sodium (DS), the chosen hydrophilic model drug, is a potent non-steroidal anti-inflammatory drug (NSAID), used in the long-term treatment of inflammation and painful conditions of rheumatic and non-rheumatic origin (Fig. 1A). DS is

Abbreviations: AMC, ammonio methacrylate copolymer; DCM, dichloromethane; DS, diclofenac sodium; DS/AMC, drug/polymer ratio; PMMA, poly(methyl methacrylate).

* Corresponding author. Tel.: +36 62 545572; fax: +36 62 545571.

E-mail address: revesz@pharm.u-szeged.hu (P. Szabó-Révész).

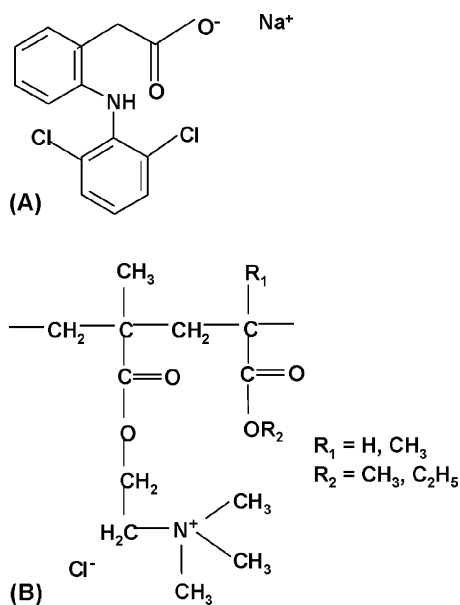


Fig. 1. Chemical structures of diclofenac sodium (DS) (a) and ammonio methacrylate copolymer (AMC) (b).

eliminated rapidly, with a half-life of 1–2 h. Hence, the rapid absorption after oral administration justifies the need for a sustained release profile. Following all routes of administration, NSAIDs exert side effects in the lower gastrointestinal tract [4]. The formulator therefore has the choice of keeping a constant drug dissolution rate or minimizing the dissolved drug concentration, i.e. the local dose of the drug in the intestine. A thermal characterization of diclofenac salts was published previously [5], and the polymorphism of DS has also been investigated [6,7]. DS-cyclodextrin solid inclusion complexes have been characterized by DSC and X-ray diffractometry (XRD) [8], and DS-containing dosage forms by IR and NMR spectroscopy [9], FT-IR spectroscopy [10,11], and Raman spectroscopy [1]. One interesting approach was the formation of a sequential interpenetrating network of polymers to produce pH-sensitive microspheres so as to investigate the molecular-level dispersion of DS, using DSC, XRD, electron microscopy and FT-IR [12].

Poly(methyl methacrylate) (PMMA) copolymers have been used as enteric coatings and sustained release coating materials in pharmaceutical technology in view of their biological safety [13,14]. The ammonio methacrylate copolymer used (AMC) (Eudragit[®] RS, Fig. 1B) is a copolymer of partial esters of acrylic and methacrylic acids with alcohols containing 5% of quaternary ammonium groups, with a chemically stable, coherent chain structure; the polymer material does not undergo any detectable change over a period of 5 years [15]. This type is the less hygroscopic Eudragit polymer, due to the low content of quaternary ammonium groups; it absorbs <5% water at 40 °C and >75% relative humidity. The AMC matrix is insoluble in water and exhibits a pH-independent permeability profile, depending on the number of positively charged quaternary ammonium groups [16,17]. PMMAs start to degrade in the side-chain at 150 °C; reactions of the main chain (depolymerisation) occur above 200 °C [15].

The thermal characterization [15,18] of the PMMA polymer and penciclovir solubility in PMMA have been reported [19], and complementary FT-IR spectroscopic examinations of AMC have also been performed [20,21]. The drug–polymer microparticles and their possible interactions have also been investigated with XRD and DSC devices, focusing on the crystallographic aspects of nicardipine–HCl [22], the dispersion state of bupivacaine [23], calculation of the enthalpy of fusion [24], and degradation of the amorphous microsphere regions [25].

With Raman or FT-Raman, the structures of PMMA-based thin organic films [26] and of PMMA-polystyrene blends [27,28], the structural modification [29], the physical aging of PMMA and the Kovacs effect [30], and the changes in intensity of PMMA upon laser irradiation [31] have been studied. The advantages of Raman include easy sample preparation and small sample need.

A specific objective of the present work was to determine an appropriate DS/AMC ratio in the microsphere preparation method for the entrapment of DS. At high-DS/AMC ratios, the quantity of the AMC may be insufficient to englobe the drug. At low ratios, DS dissolution is prevented, while the DS takes longer from the inner part to the intestinal juice. The present preformulation study is the first step towards the preparation of DS-containing microparticles.

2. Materials and methods

2.1. Materials

Micronized DS (Ph. Eur. 5) was used as hydrophilic model drug (Human Co., Hungary). Eudragit[®] RS PO (AMC) (ammonio methacrylate copolymer type B, USP/NF, Ph.Eur./NF., MW 150000) was used as matrix-forming agent (Degussa Co., Germany). The solvents dichloromethane (DCM) and ethanol (EtOH) were of reagent grade (Spectrum 3D Co., Hungary).

2.2. Methods

2.2.1. Preparation of films

The films were prepared by the solvent casting method. DS was dissolved at various DS/AMC ratios (1:12, 1:8, 1:6, 1:4 and 1:2) in EtOH and this solution was added to the AMC dissolved in DCM. The solvent mixtures, which in all examined cases were optically clear solutions, were then cast into a 10 cm Ø Teflon dish and heated at 30 °C in vacuum for 48 h. The preparation parameters of recrystallized AMC and DS materials were the same but the temperature of the vacuum dryer was 70 °C. The final transparent films were cut into disks, vacuum-dried for 24 h (Christ Alpha 1–2, Christ, Germany) and stored in a desiccator (4 °C).

2.2.2. Thermoanalytical measurements

2.2.2.1. Differential scanning calorimetry. Measurements were performed with a Mettler-Toledo DSC 821[°] instrument (Mettler Toledo, Switzerland). Accurately weighed 5.0 mg portions of the 6-month-old samples were subjected to the thermal program (–5 to 350 °C heating range; heating rate

$10\text{ }^{\circ}\text{C min}^{-1}$), in a sealed and pierced crucible under a dynamic flow of N_2 and Ar, in parallel with an empty crucible as reference. The temperatures were determined at the midpoints of the peaks.

2.2.2.2. Thermogravimetric analysis. TG analyses were performed on the individual components, physical mixtures and films in different DS/AMC ratios in platinum crucibles with the same thermal program ($25\text{--}400\text{ }^{\circ}\text{C}$ heating range; heating rate $10\text{ }^{\circ}\text{C min}^{-1}$), with a MOM Derivatograph-C (MOM Co., Hungary). The reference was a crucible containing aluminium oxide. TG (mass loss (% w/w) versus temperature), and DTG (derived mass loss vs. temperature) curves were plotted.

2.2.3. Raman microscopy measurements

The DS, AMC, and DS-containing products were characterized. Raman spectra were recorded with a Jobin Yvon LABRAM dispersion spectrometer attached to an Olympus BX41 microscope. The laser excitation wavelengths were 633 and 785 nm; better results were obtained at 785 nm, due to the lower background noise. Measurement conditions: the power on the surface of the sample was 5 mW, on a $1.1\text{ }\mu\text{m}$ diameter spot ($100\times$ magnification objective). The spectral resolution was 1.2 cm^{-1} . The back-scattered photons were dispersed on a 950 g mm^{-1} grating spot size; the acquisition time was 200–1000 s.

3. Results and discussion

3.1. Thermoanalytical measurements

3.1.1. Active pharmaceutical ingredient

The physical state of the DS in the preparation depends on its solubility in the AMC matrix and determines the DS release kinetics. The DS may be completely or partly dissolved in the AMC matrix and partly physically dispersed, depending mainly on the DS embedding method and the DS/AMC ratio. When the preparation method is suitable to dissolve the DS molecularly, a solid solution may arise. Another opportunity is the formation of metastable molecular dispersion, where the recrystallization rate of the DS depends on the viscosity of the AMC matrix and the strength of the DS–AMC interactions. A further possibility is the formation of a solid dispersion of the crystalline DS in the matrix as a DS crystal nucleus. In the solid solution form, DS–AMC interactions are the most probable cause of plasticization of the AMC. This can appear as a lowering of T_g of AMC and the absence of T_m of the DS investigated by DSC. The metastable molecular dispersion can exist under certain storage conditions for from a few days to a few years until total recrystallization [32].

When heated in the presence of air, DS decomposes below the T_m [5]; therefore the DS was subjected to thermal program in a controlled atmosphere (N_2 and Ar). The DSC curve of DS showed a sharp T_m ($293.7\text{ }^{\circ}\text{C}$) (Fig. 2). An exothermic event was observed at $308.7\text{ }^{\circ}\text{C}$, followed by an immediate decomposition effect ($323.6\text{ }^{\circ}\text{C}$). However, the shapes of the DSC curves for the initial and the recrystallized (in EtOH) DS seemed to be

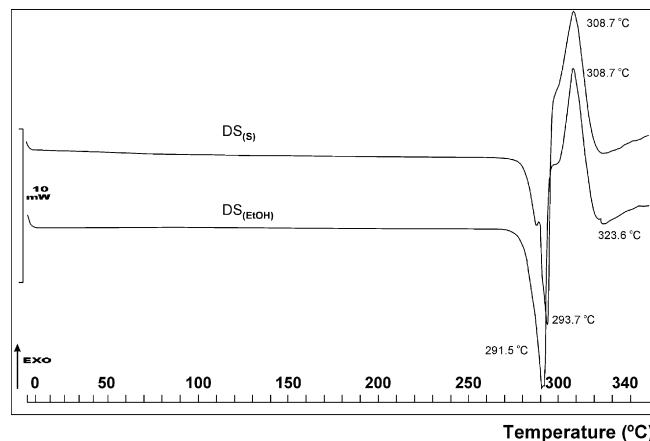


Fig. 2. DSC profile of the DS ($\text{DS}_{(s)}$, crystalline form; $\text{DS}_{(\text{EtOH})}$, recrystallized form).

the same; T_m shifted from 293.7 to $291.5\text{ }^{\circ}\text{C}$. TG analyses in air showed a mass loss of 21% in two steps between 270 and $400\text{ }^{\circ}\text{C}$, corresponding to the decomposition of DS (Fig. 3). There was a continuous mass loss due to burning from $340\text{ }^{\circ}\text{C}$ on. In the DTG curve, three peaks could be observed, at 300, 325 and $350\text{ }^{\circ}\text{C}$. In our TG measurements, no change was observed up to $270\text{ }^{\circ}\text{C}$; this can therefore be the upper limit of the spray-drying preparation method.

3.1.2. AMC and physical mixture

The DSC curve of AMC revealed three events (Fig. 4). The first endothermic peak was T_g at $65.3\text{ }^{\circ}\text{C}$. Melting of the AMC gave a broad endothermic peak at $187.2\text{ }^{\circ}\text{C}$ and a small endothermic peak at $218.4\text{ }^{\circ}\text{C}$, indicating two different crystalline part of AMC; there was no mass loss at these temperatures (Fig. 5). As a consequence, using a spray-dryer, it is not worth increasing the inlet temperature above $180\text{ }^{\circ}\text{C}$ because of the melting. The AMC decomposed above $320\text{ }^{\circ}\text{C}$. There was no mass loss up to $300\text{ }^{\circ}\text{C}$, but this was followed by a mass loss of 75% up to $400\text{ }^{\circ}\text{C}$, due to the evaporation of the decomposition fragments of AMC without burning (Fig. 5). The DTG curve showed endothermic peaks at 300, 350 and $380\text{ }^{\circ}\text{C}$. The shapes of the DSC curves for the initial and the recrystallized AMC were very similar. The endotherm peaks of T_m were the same, due to the coherent chain structure; only the T_g peak was missing, the reason being that the thermal treatment (vacuum-drying, $70\text{ }^{\circ}\text{C}$) above

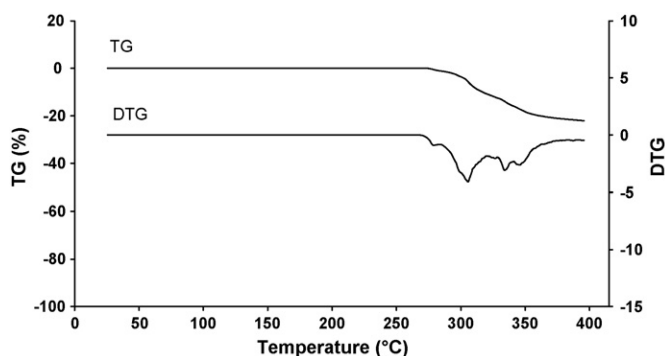


Fig. 3. TG and DTG profiles of DS (crystalline form).

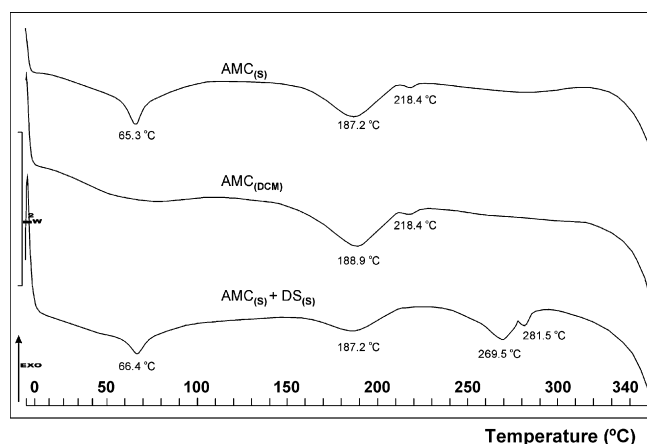


Fig. 4. DSC curves of AMC (initial and recrystallized form) and the physical mixture of AMC and DS (1:1).

T_g alters the AMC structure from a glassy to a rubbery state, and therefore the T_g event could not occur (Fig. 4).

In the physical mixture (DS/AMC ratio of 1:1), the DS could not plasticize the AMC, the T_g value of the AMC did not change significantly (by only 1 °C, from 65 to 66 °C) (Fig. 4). A diffuse melting endotherm occurred at 187.2 °C, similarly to that observed for AMC itself, while the second melting endotherm of AMC was missing, probably due to the lower mass fraction of AMC in the sample. The DS melting endotherm was observed in the thermogram at 269.5 and 281.5 °C, which revealed the existence of DS crystals. Otherwise, interactions between the melted DS and the AMC must be significant, since the DS melting point changed from 293 to 269 and 281 °C. In the TG curve, mass loss occurs in three steps, 15% from 235 to 300 °C, 27% from 300 to 360 °C, and 5% from 360 to 400 °C, due to decomposition and burning of the DS and decomposition of the AMC. Figs. 5 and 6 show the thermogravimetric profiles of AMC (initial) and the physical mixture, respectively.

3.1.3. Films with different DS/AMC ratios

On increase of DS/AMC ratio from 1:12 to 1:2, the first endotherm was observed between 50 and 55 °C, which was due to the T_g of the AMC (Fig. 7, Table 1). The area under the curve increased and T_g decreased slightly with increasing DS/AMC ratio. The melting endotherms of the AMC gradually decreased from 231 to 219 °C, in parallel with the DS/AMC ratio increasing

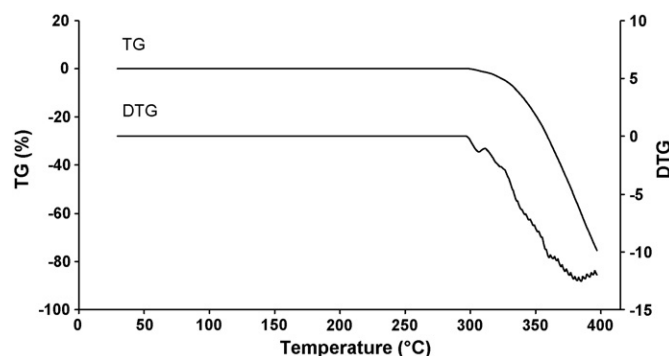


Fig. 5. TG and DTG profiles of AMC (initial form).

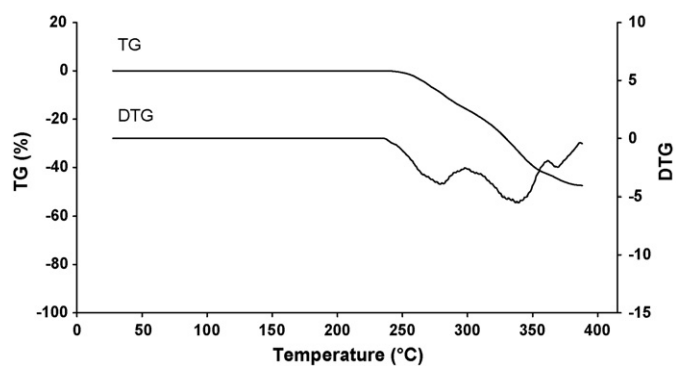


Fig. 6. TG and DTG profiles of physical mixture of DS/AMC (1:1).

from 1:12 to 1:4, but at 1:2 it increased to 228 °C. The 2 melting endotherm of AMC appeared at 1:4 DS/AMC (239 °C) and its ΔH value increased with increasing DS/AMC ratio (1:6 vs. 1:2), implying that AMC chain structure changed by the increased DS amount. At a DS/AMC ratio of 1:12/1:6, the distinctive exotherm characteristic of the DS was absent from the DSC curves because of the lack of recrystallization: the drug being in part molecularly dispersed inside the AMC matrix as a solid solution. When DS dissolves in the AMC matrix, the quaternary ammonium groups of the AMC supposedly form hydrogen bonds to the carboxylic group of the DS. The segment–segment interactions between the AMC chains are weakened by these bonds and a consequent plasticizing effect can be observed, with increased permeability, which leads to a lowered T_g value of AMC. These observations indicate that the AMC–DS complex is less prone to be crystalline than the initial AMC. The endothermic range of crystalline drug melting was noteworthy at a DS/AMC ratio of 1:2 (279 °C).

The relatively high-drug content existed in a particular dispersion state instead of a molecular dispersion, due to the reduced solubility in the polymer matrix [33], and therefore two exotherms (165 and 198 °C) appeared before the DS melting temperature. The mass was constant at these exotherm peaks. The order of magnitude of the interaction between the DS and the AMC was higher for the 1:2 DS/AMC ratio; a lower T_g was observed, from 65 °C (Fig. 4, AMC) to 50 °C (Fig. 7, DS/AMC

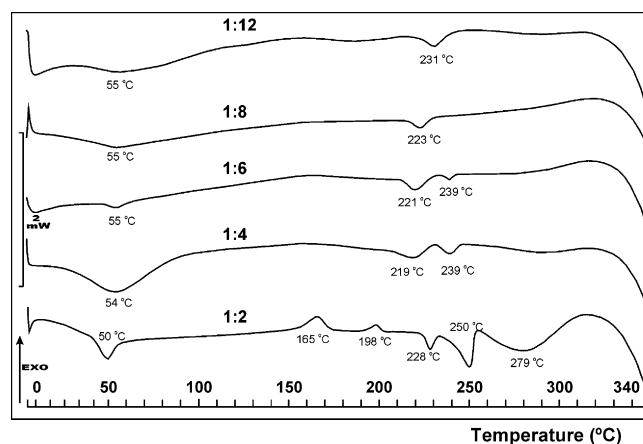


Fig. 7. DSC curves of films with DS/AMC ratios of 1:12, 1:8, 1:6, 1:4 and 1:2.

Table 1
Temperatures of peaks in DSC curves

Material	DS content (% w/w)	T_g of AMC (°C)	T_m of AMC (°C) (peak 1)	T_m of AMC (°C) (peak 2)	T_m of DS (°C) (peak 1)	T_m of DS (°C) (peak 2)
AMC (initial)	0	65	187	218	–	–
AMC (recryst.)	0	–	189	218	–	–
DS/AMC ratio, 1:12	7.6	55	231	–	–	–
DS/AMC ratio, 1:8	11.1	55	223	–	–	–
DS/AMC ratio, 1:6	14.2	55	221	239	–	–
DS/AMC ratio, 1:4	20.0	54	219	239	–	–
DS/AMC ratio, 1:2	33.3	50	228	250	279	–
Physical mixture	50	66	187	–	269	281
DS (initial)	100	–	–	–	293	308
DS (recryst.)	100	–	–	–	291	308

Table 2
Mass losses in the TG curves

Material	DS content (% w/w)	Range 1, 25–300 °C (% w/w)	Range 2, 300–400 °C (% w/w)	Total up to 400 °C (% w/w)
AMC (initial)	0	0	–75	–75
DS/AMC, 1:12	7.6	–9	–65	–74
DS/AMC, 1:8	11.1	–9	–67	–76
DS/AMC, 1:6	14.2	–10	–63	–74
DS/AMC, 1:4	20.0	–13	–56	–69
DS/AMC, 1:2	33.3	–14	–46	–60
DS (initial)	100	–3	–18	–21

ratio 1:2). Table 1 presents the temperatures of the DSC peaks versus the DS content.

In the TG curves of the DS-containing films (Figs. not shown), the processes shifted simultaneously. Table 2 presents the numerical values of the mass loss from the TG curves. They were around 0–14% (range 1) and 18–75% (range 2), which can be attributed to the decomposition and ignition of the DS and evaporation of the AMC. The mass losses of the DS-containing films were higher than expected, a possible reason being the better sublimation of the melted DS. The forces between the DS molecules were lower due to the good dispersity in the AMC matrix. The thermoanalytical measurements attracted attention to the existence of interactions between the DS and AMC.

3.2. Raman measurements

Raman measurements were carried out to confirm the physical state and possible interactions of the components. In the Raman measurements, the spectra of B–D (Fig. 8) were adjusted for the selected and characteristic band of AMC (1452 cm^{-1}) (spectrum E), to observe the principal difference between the physical mixtures (DS/AMC ratios of 1:2, 1:4 and 1:8), and the specific changes in the characteristic bands of DS between 1650 and 1570 cm^{-1} (band broadening and shift) and to confirm the existence of possible interactions. The spectra of DS (Fig. 8A), films with DS/AMC ratios of 1:2, 1:4 and 1:6 (B–D) and AMC (E) in the range 1675–1025 cm^{-1} are illustrated in Fig. 8. Spectra B–E were normalized to the 1452 cm^{-1} peak, and the intensity of spectrum A was adjusted to the peaks of the DS in spectrum B. The changes in relative intensities of the characteristic

wavenumbers of DS were due to decreasing DS content, however the difference between spectra C and D did not prove the double drug amount. The changes in the phenyl and carbonyl vibrations of the DS in the region 1630–1550 cm^{-1} differed in spectra B–D, which is in accordance with the literature [34,35], the band at 1590 cm^{-1} is not distinct from the 1581 cm^{-1} peak, but forms a shoulder (Fig. 8.). The shoulder at 1163 cm^{-1} had disappeared, while the band had become broader. In the presented spectra, the traces of crystalline DS could be identified, which was in accord with the DSC results. The selected Raman bands of the DS, AMC and three representative films with their vibrational assignments (cm^{-1}) are presented in Table 3.

Table 3 and Fig. 8 clearly reveal dominant bands of DS. Sharp peaks at 1049 and 1075 cm^{-1} are attributed to the ring 2 (phenylacetate) and ring 1 (dichlorophenyl) breathing. Medium sharp peaks at 1238 and 1283 cm^{-1} are attributed to the C–N–C and

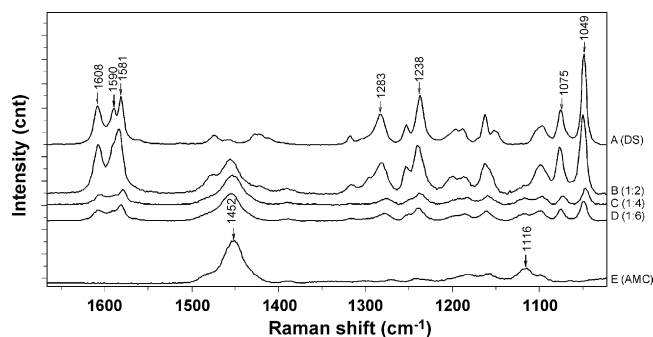


Fig. 8. Raman spectra of DS (A) and films with DS/AMC ratios of 1:2 (B), 1:4 (C), 1:6 (D) and AMC (E).

Table 3
Raman bands in the spectra

DS	AMC	DS/AMC 1:2	DS/AMC 1:4	DS/AMC 1:6	Vibrational assignment
1049 s	–	1048 s	1046 w	1049 w	Ring 2 breathing
1075 m	–	1076 m	1073 w	1075 w	Ring 1 breathing
1094 mw	–	1094 mw	1092 mw	1093 mw	CH-wag + CH bend. (rings)
–	1116w	1118 sh	1118 w	1118 w	CO-str. coupled with methyl rocking
1162 ^a m	1160 ^a w	1162 m	1160 w	1162 w	CH bend. (rings) Carbonyl str. (ester group) ^a
1238 s	–	1240 s	1238 w	1238 w	C–N–C symmetric str. + CH rock (ring 1 + 2)
1252 sh	–	1253 sh	–	1252 sh	C6–(ring 2)–CH ₂ str. + CH rock (ring 1 + 2)
1283 m	–	1280 m	1276 w	1279 w	CH rock (ring 1 + 2) and R-CO.OR' asymmetric str.
–	1452 m	1455 m	1452m	1454 m	CH ₂ -symmetric bend./deformation
1581 s	–	1583 s	1578 w	1582 w	O ¹ C ⁸ O ² asymmetric str.
1590 sh	–	1590 sh	–	1590 sh	Ring 1 str.
1608 m	–	1606 ms	1605 w	1608 w	Ring 2 str.
–	1736 m (in Fig. 9)	Not scanned	Not scanned	1736 m (in Fig. 9)	Carbonyl group of the trimethyl–ammonioethyl methacrylate segment

Abbreviations: w, weak; m, medium; s, strong; sh, shoulder; bend, bending; ring 1, dichlorophenyl ring; ring 2, phenylacetate ring; str, stretching; wag, wagging.

^a Vibrational assignment.

rings 1–2 stretching. The three characteristic peaks at 1581, 1590 and 1608 cm⁻¹ are due to the O¹C⁸O² asymmetric stretching and to rings 1 and 2 stretching vibrations, respectively. In the spectrum of AMC, two characteristic peaks of C–O stretching and the CH₂-symmetric bending at 1116 and 1452 cm⁻¹, respectively, can be seen (Fig. 8). The increases in the bandwidths at the DS/AMC ratio of 1:2 mean a decrease in the vibrational relaxation time due to the weak interaction of O¹C⁸O² of DS with the quaternary ammonium group of AMC. To observe the changes in the peak shapes and positions in the overlapping regions required subtraction of the spectra from each other. According to the DSC measurements, the film with a DS/AMC ratio of 1:6 contained less crystalline DS, and it was therefore chosen to prepare the difference spectra and analyse them. The spectrum of the DS (Fig. 9D) was subtracted from the spectrum of the film with a DS/AMC ratio of 1:6 (Fig. 9A), and the result (Fig. 9C) was compared with the spectrum of AMC (Fig. 9B). The Raman spectrum of AMC did not change within A and B (Fig. 9C). There was no difference in the lines of AMC between spectra B and C. In the marked regions (1650–1530 cm⁻¹, 1300–1250 cm⁻¹, 1150–1050 cm⁻¹ and 570–200 cm⁻¹), the differences arose from the changes in DS content. For determination of the changes in DS, the difference spectrum of the

model mixture (A) and AMC (B) was calculated. The result (E) was compared with the DS spectrum (D); the differences could be well observed in the regions overlapping with AMC bands (1500–1400 cm⁻¹ and 850–800 cm⁻¹). The intensity ratio of the peaks of DS/AMC ratios between 1120 and 1030 cm⁻¹ was 1:1:6, the intensity of 1:2 ratio was higher. The peak at 442 cm⁻¹ (D) was shifted to 450 cm⁻¹ and its left shoulder had disappeared. A significant intensity increase and shape alteration could be observed in the group around 300 cm⁻¹. Merging of the broadening peaks at 247–241 cm⁻¹ and 225 cm⁻¹ also occurred. There were no significant difference in the characteristic peak of the carbonyl group of the AMC (1736 cm⁻¹) (Fig. 9), which belongs to the trimethyl–ammonioethyl methacrylate segment; it was in accordance with Fujimori et al. [20]. This confirmed that the strength of possible interaction between the carbonyl group of AMC and the DS decreased at DS/AMC ratio of 1:6. The changes between D and E indicate that the crystalline state of DS was changed, while the broadening and merging effects suggest partly molecular dispersity for the DS.

4. Conclusions

If microspheres are prepared, using the multiple emulsion–solvent evaporation technique, due to the more successful distribution of the drug molecules inside the polymer matrix, the drug could have a better possibility to be in a molecular dispersion form. The successful formulation of a stable and effective dosage form also depends on the amount of the drug and the strength of the possible interactions, because interactions between drug and polymer could promote the release and protect the connections of the drug molecules in the polymer matrix. From this work, the following conclusions and implications can be drawn:

- According to the DSC results, DS is either partly molecularly dispersed or entirely dissolved in the investigated films.

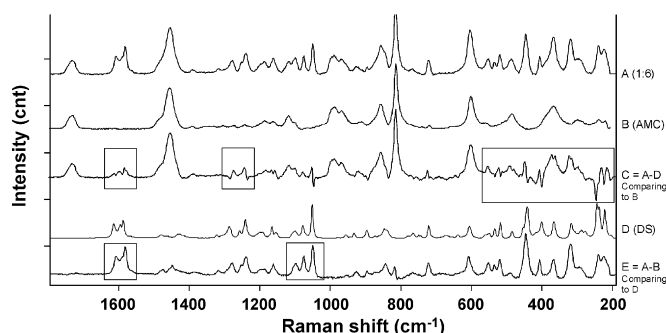


Fig. 9. Raman spectra of film (DS/AMC ratio of 1:6 A), AMC (B), film minus DS (C), DS (D) and film minus AMC (E).

At lower DS content, there was an absence of the main characteristic thermal events of DS, and its partial molecular dispersion in the AMC matrix was ensured. As the DS content was increased to about 20% (w/w) (DS/AMC ratio of 1:4), the drug particles could increasingly be in contact with each other, indicating the crystalline state of DS and plasticization of AMC. A partial solid solution of DS was formed at DS/AMC ratios of 1:12, 1:8 and 1:6; it was mainly crystalline at a ratio of 1:4, while it remained crystalline at a ratio of 1:2. The formulator should use a sensitive balance between the two main DS dispersity types as a valuable tool. The molecular dispersion of DS ensures a higher dissolution rate in the intestinal juice, but in the crystalline state, when the DS diffuses out of the matrix, leaving channels, this phenomenon could increase the drug dissolution rate to such an extent that this rate could exceed the required sustained release rate. No significant difference was revealed by any major structural change, except for the effects of the different DS contents of the measured films.

- (ii) Raman measurements were carried out to confirm the interactions of the components (DS/AMC ratio of 1:6). The numerous peaks in the Raman spectra were indicative of the chemical compositions and structures of the drug and polymer and confirmed that the DS and AMC were compatible with each other. There were only small changes, such as broadening and shifting of the peaks corresponding to the $O^1C^8O^2$ ions of DS (1581 cm^{-1}) and the quaternary ammonium groups of AMC ($900\text{--}800\text{ cm}^{-1}$), indicating the decrease in the vibrational relaxation time. The dichlorophenyl ring stretching of DS (1590 cm^{-1}) was missing, which could otherwise indicate an ionic interaction, but in addition, the strength of the possible interactions between the DS and AMC chains could not be enough to have an additional retaining effect of the drug from dissolution. These investigations facilitate the selection of the appropriate DS/AMC ratio in the preformulation study of the microsphere preparation process, in conformity with the therapeutic aim.

Acknowledgements

The authors thank György Marosi (Department of Organic Chemical Technology, Budapest University of Technology and Economics) for his kind help in the measurements with the Raman spectrometer. This work was supported by the Hungarian National Fund, OTKA (project no. T046908).

References

- [1] S. Mazurek, R. Szostak, *J. Pharm. Biomed. Anal.* 40 (2006) 1235–1242.

- [2] A. Szép, A. Szabó, N. Tóth, P. Anna, Gy. Marosi, *Polym. Degrad. Stabil.* 91 (2006) 593–599.
- [3] B.M. Murphy, S.W. Prescott, I. Larson, *J. Pharm. Biomed. Anal.* 38 (2005) 186–190.
- [4] M. Petruzzelli, M. Vacca, A. Moschetta, R.C. Sasso, G. Palasciano, K.J. Erpecum, P. Portincasa, *Clin. Biochem.* 40 (2007) 503–510.
- [5] F. Giordano, A. Rossi, I. Pasquali, R. Bettini, E. Frigo, A. Gazzaniga, M.E. Sangalli, V. Mileo, S. Catinella, *J. Therm. Anal. Calorim.* 73 (2003) 509–518.
- [6] C. Castellari, S. Ottani, *Acta Crystallogr. C53* (1997) 794–797.
- [7] N. Jaiboon, K. Yos-in, S. Ruangchaithaweesook, N. Chaichit, R. Thutivoranath, K. Siraleartmukul, S. Hannongbua, *Anal. Sci.* 17 (2001) 1465–1466.
- [8] B. Pose-Vilarnovo, C.R.-T. Sánchez, N.D. Moure, J.L. Vila-Jato, J.J. Torres-Labandeira, *J. Therm. Anal. Calorim.* 73 (2003) 661–670.
- [9] I.M. Kenawi, B.N. Barsoum, M.A. Youssef, *J. Pharm. Biomed. Anal.* 37 (2005) 655–661.
- [10] O. Şanlı, N. Ay, N. Işıkkan, *Eur. J. Pharm. Sci.* 65 (2007) 204–214.
- [11] M. Bartolomei, P. Bertocchi, E. Antoniella, A. Rodomonte, *J. Pharm. Biomed. Anal.* 40 (2006) 1105–1113.
- [12] M.D. Kurkuri, T.M. Aminabhavi, *J. Control Release* 96 (2004) 9–20.
- [13] M.L. González-Rodríguez, F. Maestrelli, P. Mura, A.M. Rabasco, *Eur. J. Pharm. Sci.* 20 (2003) 125–131.
- [14] S. Narisawa, M. Nagata, Y. Hirakawa, M. Kobayashi, H. Yoshino, *J. Pharm. Sci.* 85 (1996) 184–188.
- [15] H.-U. Petereit, W. Weisbrod, *Eur. J. Pharm. Biopharm.* 47 (1999) 15–25.
- [16] S. Haznedar, B. Dortunç, *Int. J. Pharm.* 269 (2004) 131–140.
- [17] Eudragit, Technical Information, RöhmPharma, Darmstadt, Germany, 2001.
- [18] A. Kramar, S. Turk, F. Vrečer, *Int. J. Pharm.* 256 (2003) 43–52.
- [19] A. Ahmed, B.W. Barry, A.C. Williams, A.F. Davis, *J. Pharm. Biomed. Anal.* 34 (2004) 945–956.
- [20] J. Fujimori, Y. Yoshihashi, E. Yonemochi, K. Terada, *J. Control Release* 102 (2005) 49–57.
- [21] O. Sipahigil, A. Gürsoy, F. Çakalağaoğlu, İ. Okar, *Int. J. Pharm.* 311 (2006) 130–138.
- [22] N. Yuksel, T. Tincer, T. Baykara, *Int. J. Pharm.* 140 (1996) 145–154.
- [23] P. LeCorre, P. LeGuevello, V. Gajan, F. Chevanne, R. LeVerge, *Int. J. Pharm.* 107 (1994) 41–49.
- [24] W.-J. Lin, C.-C. Yu, *J. Microencapsulat.* 19 (6) (2002) 767–773.
- [25] U. Edlund, A.-C. Albertsson, *Adv. Polym. Sci.* 157 (2002) 67–112.
- [26] R. Cristescu, G. Socol, I.N. Mihailescu, M. Popescu, F. Sava, E. Ion, C.O. Morosanu, I. Stamantin, *Appl. Surf. Sci.* 208–209 (2003) 645–650.
- [27] A. Matsushita, Y. Ren, K. Matsukawa, H. Inoue, Y. Minami, I. Noda, Y. Ozaki, *Vib. Spectrosc.* 24 (2000) 171–180.
- [28] C. Li, Y. Shi, Z. Fu, *Polym. Int.* 55 (2006) 25–30.
- [29] H.W. Choia, H.J. Wooa, W. Honga, J.K. Kima, S.K. Leeb, C.H. Euma, *Appl. Surf. Sci.* 169 (2001) 433–437.
- [30] A. Wypych, E. Duval, A. Mermet, G. Boiteux, L. David, J. Ulanski, S. Etienne, *J. Non-Cryst. Solids* 352 (2006) 4562–4567.
- [31] E. Rebolgar, G. Bounos, M. Oujja, C. Domingo, S. Georgiou, M. Castillejo, *Appl. Surf. Sci.* 248 (2005) 254–258.
- [32] C. Dubernet, *Thermochim. Acta* 248 (1995) 259–269.
- [33] S. Freiberg, X.X. Zhu, *Int. J. Pharm.* 282 (2004) 1–18.
- [34] T. Iliescu, M. Baia, V. Miclăuş, *Eur. J. Pharm. Sci.* 22 (2004) 487–495.
- [35] T. Iliescu, M. Baia, W. Kiefer, *Chem. Phys.* 298 (2004) 167–174.